CONF-901010--2
PNL-SA-18155

PNL-SA--18155

DE91 005107

STATISTICAL UNCERTAINTY ANALYSIS OF RADON TRANSPORT IN NONISOTHERMAL, UNSATURATED SOILS

October 1990

D. J. Holford
P. C. Owczarski
G. W. Gee
H. D. Freeman

Presented at the
Twenty-Ninth Hanford Symposium on
Health and the Environment
Richland, Washington
October 16-19, 1990

Work supported by
the U. S. Department of Energy
under Contract DE-AC06-76RLO 1830

Pacific Northwest Laboratory
Richland, Washington 99352

STATISTICAL UNCERTAINTY ANALYSIS OF RADON TRANSPORT IN NONISOTHERMAL, UNSATURATED SOILS

D. J. Holford, P. C. Owczarski, G. W. Gee, H. D. Freeman

P.O. Box 999

Pacific Northwest Laboratory, Richland, Washington 99352

INTRODUCTION

To accurately predict radon fluxes from soils to the atmosphere, we must know more than the radium content of the soil. Radon flux from soil is affected not only by soil properties, but also by meteorological factors such as air pressure and temperature changes at the soil surface, as well as the infiltration of rainwater. Natural variations in meteorological factors and soil properties contribute to uncertainty in subsurface model predictions of radon flux, which, when coupled with a building transport model, will also add uncertainty to predictions of radon concentrations in homes. A statistical uncertainty analysis using our Rn3D finite-element numerical model was conducted to assess the relative importance of these meteorological factors and the soil properties affecting radon transport.

RADON TRANSPORT IN NONISOTHERMAL, UNSATURATED SOILS

The Rn3D model has been enhanced to simulate the nonisothermal transport of radon by diffusion and advection in both the liquid (water) and the gas (air) phase. This three-dimensional finite-element code was used to simulate the effect of air pressure, water pressure, and temperature gradients on radon concentration in partially saturated soil with parallel, partially penetrating cracks. For this uncertainty analysis, a two-dimensional steady-state scenario was assumed, as shown in Figure 1.

Using Einstein's summation convention, steady-state two-phase transport of radon in partially saturated soil is governed by

$$\frac{\partial}{\partial x_i}\left(D_{ij}\frac{\partial C_a}{\partial x_j}\right) - \frac{\partial}{\partial x_i}\left[\frac{v_{a_i} - v_{w_i}\kappa}{\varepsilon(1-s+s\kappa)} C_a\right] - \lambda C_a + \frac{R\rho_b\lambda E/n}{1-s+s\kappa} = 0 \quad (1)$$

where C_a = concentration of radon in air-filled pore space,

D = bulk diffusion coefficient of radon in partially saturated soil,

v_a = Darcy velocity of air,

v_w = Darcy velocity of water,

κ = solubility coefficient of radon in water relative to air,

ε = soil porosity,

s = percent saturation of the soil pore space with water,

λ = radon-222 decay coefficient,

R = radium content of the soil,

ρ_b = bulk density of the soil,

E = radon emanation coefficient, and

i and j = directional indices of the Cartesian coordinate system.

The Darcy velocity of air is given by

$$v_{a_i} = -\frac{k_{a_{ij}}}{\mu_a}\left(\frac{\partial p_a}{\partial x_j} + \rho_a g\frac{\partial z}{\partial x_j}\right) \quad (2)$$

where k_a = permeability of the air phase (in units of length squared),

p_a = air phase pressure,

μ_a = dynamic viscosity of air, and

z = vertical distance above an arbitrary datum.

Similarly, the Darcy velocity of water is given by

$$v_{w_i} = - \frac{k_{w_{ij}}}{\mu_w} \left(\frac{\partial p_w}{\partial x_j} + \rho_w g \frac{\partial z}{\partial x_j} \right) \tag{3}$$

where k_w = permeability of the water phase (in units of length squared), p_w = water phase pressure, and μ_w = dynamic viscosity of water.

Several of the model variables are dependent on soil pore saturation with water. The capillary pressure of partially saturated soil is defined as the difference between the water and the air phases, and is related to matric suction by the density of water and gravitational acceleration

$$p_c = p_a - p_w = -\psi \rho_w g \tag{4}$$

where p_c = capillary pressure,

ψ = matric suction,

ρ_w = density of water, and

g = gravitational acceleration.

The matric suction is related to the saturation by the following empirical relation (van Genuchten 1980):

$$\frac{s - s_r}{s_w - s_r} = \left[\frac{1}{1 + (\alpha \psi)^n} \right]^m \tag{5}$$

where s_r = residual water saturation,

s_w = maximum water saturation,

n = empirical constant correlated with pore size distribution,

$m = 1-2/n$, and

α = inverse of the air-entry pressure.

The values of n, m, and α were obtained for three different soils by fitting the van Genuchten model to measured water retention data from a catalogue of soils (Mualem 1976a).

The permeability of the water phase can be predicted using the variables n and m from Equation 5 (Mualem 1976b):

$$k_w = k\, s^{\xi}\left[1 - \left(1 - s^{1/m}\right)^m\right]^2 \tag{6}$$

where k = intrinsic permeability and ξ = exponent commonly fixed at 0.5. The permeability of the air phase was assumed to be related to the water permeability by

$$k_a = k\,(1 - k_w)(1 - s)^2 \tag{7}$$

The bulk diffusion coefficient for radon in partially saturated soil was calculated as a function of water saturation using

$$D_{ij} = \tau_{ij}\left\{\frac{D_a}{\left[1+\frac{s\kappa}{(1-s)}\right]^{\chi}} + \frac{D_w}{1+\frac{(1-s)}{s\kappa}}\right\} \tag{8}$$

where τ = tortuosity factor for a soil,

D_a = diffusion coefficient of radon in pure air,

D_w = diffusion coefficient of radon in pure water, and

χ = an exponent set, in this case, to four.

If χ is set equal to one, Equation 8 represents the bulk diffusion coefficient of radon in partially saturated soil, assuming no pore blockage occurs until a pore fills with water (Nielson et al. 1984). In reality, pore blockage occurs before a pore is completely filled. Setting χ to four provides a better fit to data measured by (Nielson et al. 1984).

The emanating fraction of radon from the soil was calculated from

$$E = \begin{cases} E_w s/s^* + E_a(1 - s/s^*) & s < s^* \\ E_w & s > s^* \end{cases} \tag{9}$$

where E_w and E_a = emanation coefficients at saturation and at dryness, and s^* = minimum moisture on the plateau of an emanation-versus-moisture curve (Nielson et al. 1984).

The properties of water and air are treated as functions of temperature and pressure in Rn3D. The viscosity of water, viscosity of air, and density of water as functions of temperature were implemented tabular functions for temperatures between 0 and 100°C (Weast 1982). The density of air as a function of temperature and pressure was calculated from the ideal gas law (Weast 1982):

$$\rho_a = \left(\frac{1.293}{1 + 0.00367\ T}\right)\left(\frac{p}{1333.224 * 76}\right) \tag{10}$$

where ρ_a = density of dry air (kg/m^3), T = temperature (°C), and p = absolute pressure (Pa).

The diffusion of radon in pure water was calculated as a function of temperature (Bird et al. 1960; Hart 1986):

$$D_w = 7.4\text{x}10^{-12}\ \frac{(T+273.15)\sqrt{\varphi_w M_w}}{(\mu_w)\left(M_{Rn}/\rho_{Rn}\right)^{0.6}} \tag{11}$$

where D_w = diffusion of radon in pure water (m^2/s),

T = temperature (°C),

φ = "association parameter" for water given as 2.6,

M_w = molecular weight of water,

μ_w = viscosity of water as a function of temperature (centipoise),

M_{Rn} = molecular weight of radon, and

ρ_{Rn} = density of radon at the normal boiling point given as 4.4x10^3 kg/m^3 (Herreman 1980).

The diffusion of radon in pure air was calculated as a function of temperature and pressure (Bird et al. 1960):

$$D_a = \frac{3.640\text{x}10^{-8}}{1.01325\text{x}10^7\ p}\left(\frac{T + 273.15}{\sqrt{T_{cRn}T_{ca}}}\right)^{2.334}(100\,p_{cRn}p_{ca})^{1/3}(T_{cRn}T_{ca})^{5/12}\left(\frac{1}{M_{Rn}} + \frac{1}{M_a}\right) \tag{12}$$

where D_a = diffusion of radon in pure air (m^2/s),

T = temperature (°C),

p = absolute pressure (Pa),

T_{cRn} = critical temperature of radon (°K),

T_{ca} = critical temperature of air (°K),

p_{cRn} = critical pressure of radon (Pa),

p_{ca} = critical pressure of air (Pa), and

M_a is the molecular weight of air.

The diffusion coefficients calculated in this manner show good agreement with compiled data (Hart 1986).

The solubility of radon in water/air at atmospheric pressure was implemented as a tabular function of temperatures between 0 and 100°C (Table 1).

Table 1. Solubility of Radon in Water/Air at Atmospheric Pressure

T (°C)	K
0	0.507
10	0.340
10	0.250
30	0.195
37	0.167
50	0.138
75	0.114
100	0.106

STATISTICAL UNCERTAINTY ANALYSIS

If some input variables are very influential on Rn3D's prediction of radon flux to the atmosphere, those input variables should be measured at field sites with the highest degree of spatial and temporal accuracy. An uncertainty analysis attempts to quantify the uncertainty of model output, giving an indication of the probable range of possible outcomes. A schematic diagram (Figure 2) shows the statistical method used to perform this uncertainty analysis. Each input variable was treated as a random variable, with a certain range and a uniform, loguniform, normal, or lognormal distribution (Table 2).

Table 2. Input Variables, Their Ranges and Distributions

Variable	Range	Units	Distribution
atmospheric radon	0.1 to 100	Bq/m^3	loguniform
atmospheric pressure	8.5×10^4 to 10^5	Pa	uniform
capillary pressure	10^3 to 5×10^4	Pa	loguniform
gas pressure gradient	10^{-3} to 1	Pa/m	loguniform
liquid pressure gradient	10^{-1} to 10^2	Pa/m	loguniform
temperature gradient	-0.9 to 0.5	°C / m	uniform
intrinsic permeability	± 1 order mag.	m^2	lognormal
porosity	± 5%	---	normal
tortuosity	± 10%	---	normal
radium content	10 to 200	Bq/kg	loguniform
crack width	10^{-4} to 10^{-2}	m	loguniform
crack depth	0.3 to 6	m	loguniform
crack spacing	0.6 to 20	m	loguniform
water table depth	-30 to -10	m	uniform

Latin Hypercube Sampling (Iman and Shortencarier 1984) was used to select random combinations of the model input variables within the ranges listed in Table 2. Each random combination of input variables was used for one run of Rn3D. A suite of such runs composes a Monte Carlo simulation (Hammersley and Handscomb 1964). The advantage of Latin Hypercube Sampling is that, rather than running the model many times (as with the traditional Monte Carlo technique), the model must be run only two or three times the number of input variables.

Most of the input variables were given either uniform or loguniform distributions to evenly sample their entire ranges. The soil properties permeability, porosity, and tortuosity were assumed to be less uncertain than the rest of the input variables, and were given normal or lognormal distributions. In addition, the moisture characteristic curves, relative permeability, diffusion-versus-moisture and emanation-versus-moisture curves were assumed to be known for three soil types. These four curves are shown in Figures 3,4,5, and 6, respectively, where moisture content is defined as the product of soil saturation (s) and porosity (ϵ). Three Monte Carlo simulations, each consisting of 35 runs of Rn3D, were conducted for these three soils: sand, loam, and clay in order to assess uncertainties for different soil types. The base case soil properties for each of the three Monte Carlo simulations are listed in Table 3.

Table 3. Base Case Soil Properties for Three Monte Carlo Simulations

Property	Sand	Loam	Clay
permeability (m^2)	$1x10^{-10}$	$1x10^{-13}$	$1x10^{-16}$
porosity	0.2526	0.4491	0.5631
tortuosity	0.6	0.4	0.2
van Genuchten (Mualem)			
residual saturation	0.1229	0.2299	0.5409

n	4.886	2.502	1.8133
alpha (m^{-1})	2.37	1.66	0.83
emanation			
wet	0.3	0.3	0.3
dry	0.1	0.1	0.1
minimum saturation	0.3	0.4	0.6

Figure 7 is a probability plot of the results of the three Monte Carlo simulations. The predicted radon flux varies over five orders of magnitude. Interestingly, the variability between soil types is much less than the total variability for each soil type.

SENSITIVITY ANALYSIS

The results of the Monte Carlo simulations can be used to determine the sensitivity of the radon flux to each input variable, expressed as sensitivity coefficients. The sensitivity coefficient represents the percentage change in flux that results from a percentage change in an input variable:

$$a_i = \frac{dF/F}{dX_i/X_i} = \frac{d(\ln F)}{d(\ln X_i)} \tag{13}$$

where a_i = sensitivity coefficient, F = total radon flux from the soil to the atmosphere, and X_i = i^{th} input variable.

The sensitivity coefficients can be estimated using multiple linear regression, by assuming a first-order model for the relationship between the radon flux and the input variables:

$$\ln\hat{F} = \hat{a}_0 + \hat{a}_1 \ln X_1 + \hat{a}_2 \ln X_2 + \cdots + \hat{a}_k \ln X_k \tag{14}$$

where $\hat{a}_i$ = i^{th} regression coefficient (estimated sensitivity coefficient) and k is the number of input variables.

The sensitivity coefficient can be standardized so that input variables with widely varying ranges can be compared:

$$\hat{a}_i^* = \hat{a}_i / \sigma_{\hat{a}_i} \quad (15)$$

where $\hat{a}_i^*$ = standardized sensitivity coefficient and $\sigma_{\hat{a}_i}$ = standard deviation of the sensitivity coefficient. This standardized sensitivity coefficient is regarded to be significant if its absolute value is larger than two (representing variability larger than two standard deviations of the sensitivity coefficient). A negative coefficient indicates that the radon flux increases as the input variable's value decreases; a positive coefficient indicates the converse.

The standardized sensitivity coefficients for the three Monte Carlo simulations are shown in Figures 8, 9 and 10. Input variables that have standardized sensitivity coefficients larger than two are

- width of cracks (or other macropores)
- radium content
- gas pressure gradient
- capillary pressure (soil saturation).

Variables with sensitivity coefficients between one and two, and which are therefore marginally significant, are

- permeability
- atmospheric pressure
- depth to water table
- crack spacing.

The differences in sensitivity coefficients calculated for the different soil types are not great, although some trends are apparent. For instance, the sensitivity coefficient for crack width is larger for a clay than for a sand, because of the larger permeability contrast between cracks in a low-permeability clay than in a high-permeability sand. For the same reason, the clay soil scenario is more sensitive to variations in the soil permeability than is the sand scenario. Because of higher gas velocities, the gas pressure gradient is a more significant factor in the higher-permeability sand simulations.

CONCLUSIONS

This analysis indicates several input variables to the Rn3D model that should be carefully measured to accurately predict radon fluxes from soils. Obviously nondestructive field measurements of crack width, spacing, and depth are not practical. But the sensitivity of radon flux to the presence of cracks in the soil suggests that using the laboratory-measured properties of a small soil sample to predict radon fluxes into a house is an insufficient technique if cracks are indeed present. Field methods for measuring the bulk permeability and porosity of a large, in situ soil sample are necessary to accurately predict the radon gas transport properties of the soil.

Future work will include sensitivity and uncertainty analyses of more realistic scenarios with time-varying atmospheric pressure, temperature, and rainfall. In these cases, neither the pressure and temperature gradients, nor the soil saturation will be uniform in the soil.

REFERENCES

Bird, R. B., W. E. Stewart and E. N. Lightfoot. (1960). Transport Phenomena. John Wiley & Sons, New York, NY.

Hammersley, J. M. and D. C. Handscomb. (1964). Monte Carlo Methods. Methuen, London, England.

Hart, K. P. (1986). Radon Exhalation from Uranium Tailings, Volume 1. Ph.D. Thesis. University of New South Wales, Kensington, N.S.W.

Herreman, W. (1980). "Calculation of the Liquid Density of Radon." Cryogenics. 20(3): 133-134.

Iman, R. L. and M. J. Shortencarier. (1984). A FORTRAN 77 Program and User's Guide for the Generation of Latin Hypercube and Random Samples for Use with Computer Models. NUREG/CR-3624, SAND83-2365. Sandia National Laboratories, Albuquerque, New Mexico.

Mualem, Y. (1976a). A Catalogue of the Hydraulic Properties of Soils. Research Progress Report 442. Technion, Israel Institute of Technology, Haifa, Israel.

Mualem, Y. (1976b). "A New Model for Predicting the Hydraulic Conductivity of Unsaturated Porous Media." Water Resour. Res. 12: 513-522.

Nielson, K. K., V. C. Rogers and G. W. Gee. (1984). "Diffusion of Radon through Soils: A Pore Distribution Model." Soil Sci. Soc. Am. J. 48(3): 482-487.

van Genuchten, M. T. (1980). "A Closed-Form Equation for Predicting the Hydraulic Conductivity of Unsaturated Soils." Soil Sci. Soc. Am. J. 44: 892-898.

Weast, R. C. (1982). CRC Handbook of Chemistry and Physics. CRC Press, Inc., Boca Raton, Florida.

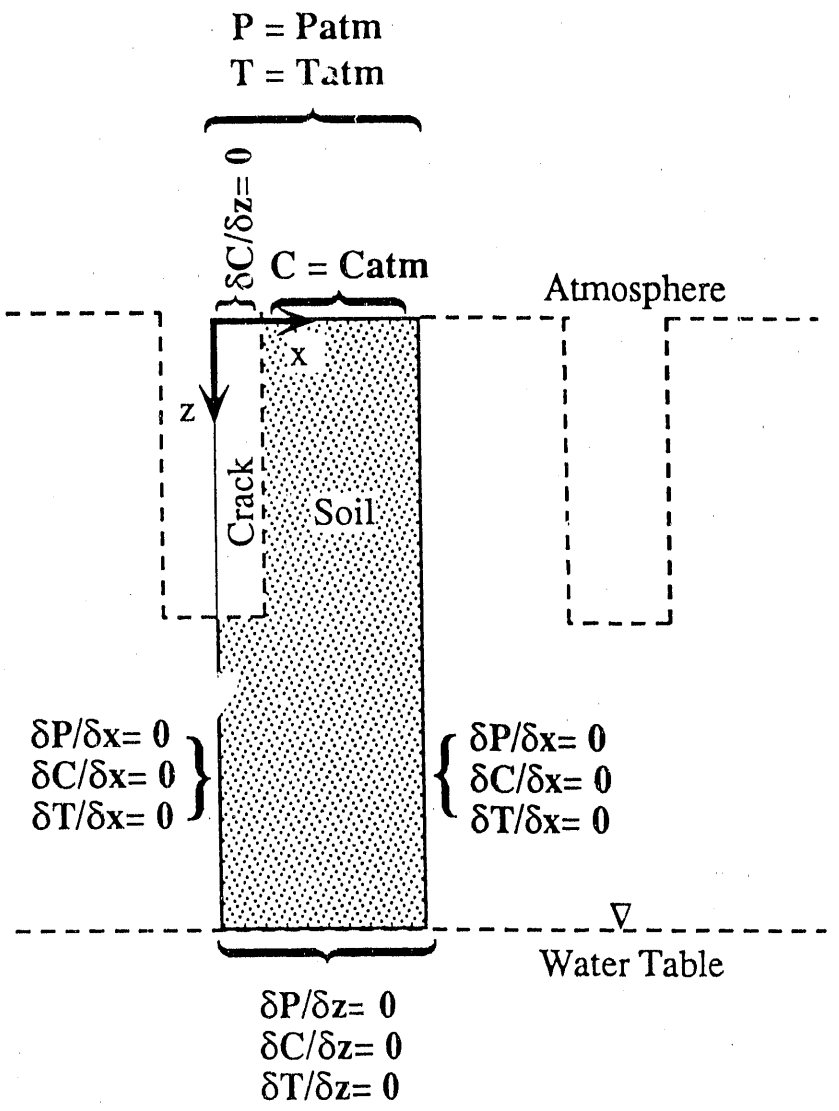
P = Patm
T = Tatm
δC/δz= 0
C = Catm
Atmosphere
x
z
Crack
Soil
δP/δx= 0
δC/δx= 0
δT/δx= 0
δP/δx= 0
δC/δx= 0
δT/δx= 0
Water Table
δP/δz= 0
δC/δz= 0
δT/δz= 0

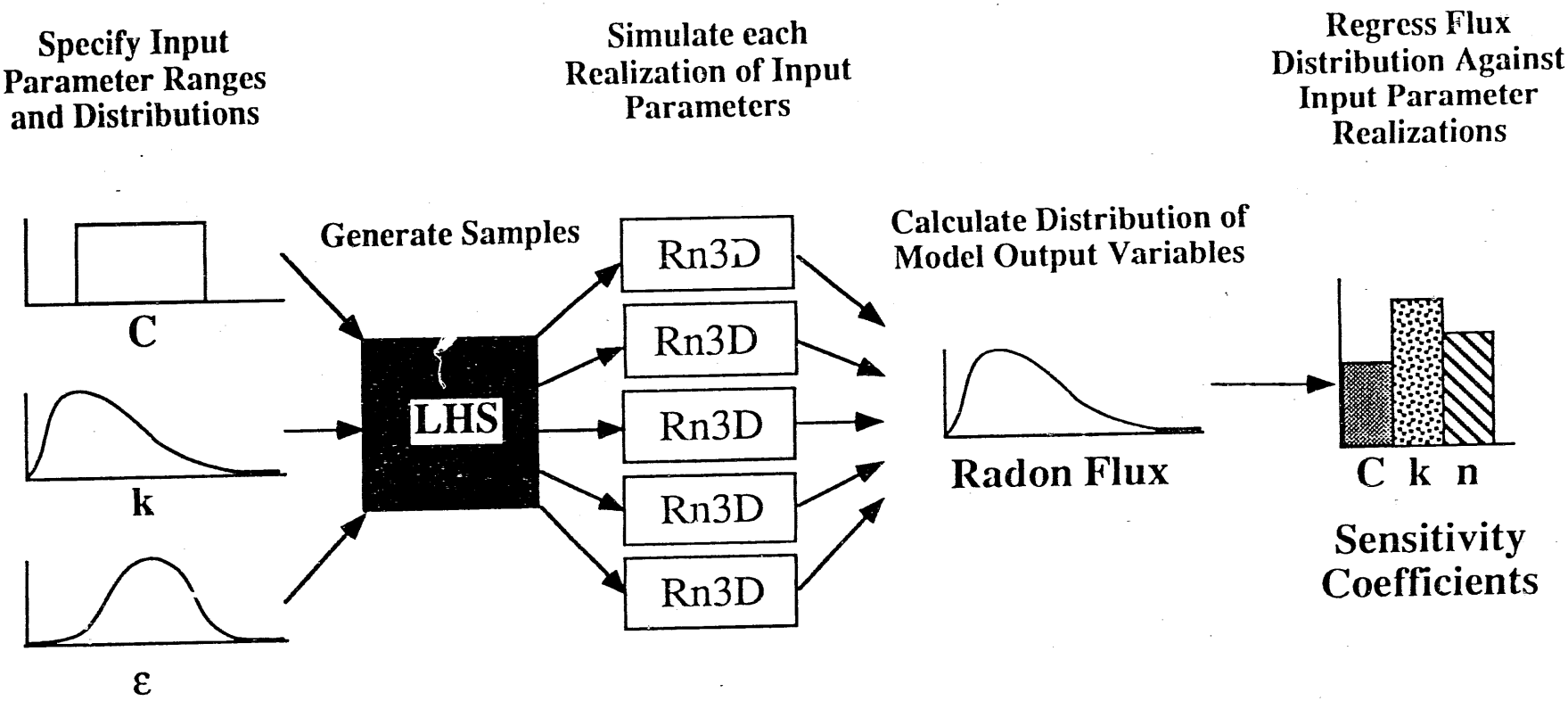
Specify Input Parameter Ranges and Distributions
Simulate each Realization of Input Parameters
Regress Flux Distribution Against Input Parameter Realizations
Generate Samples
C
k
ε
LHS
Rn3D
Rn3D
Rn3D
Rn3D
Rn3D
Calculate Distribution of Model Output Variables
Radon Flux
C k n
Sensitivity Coefficients

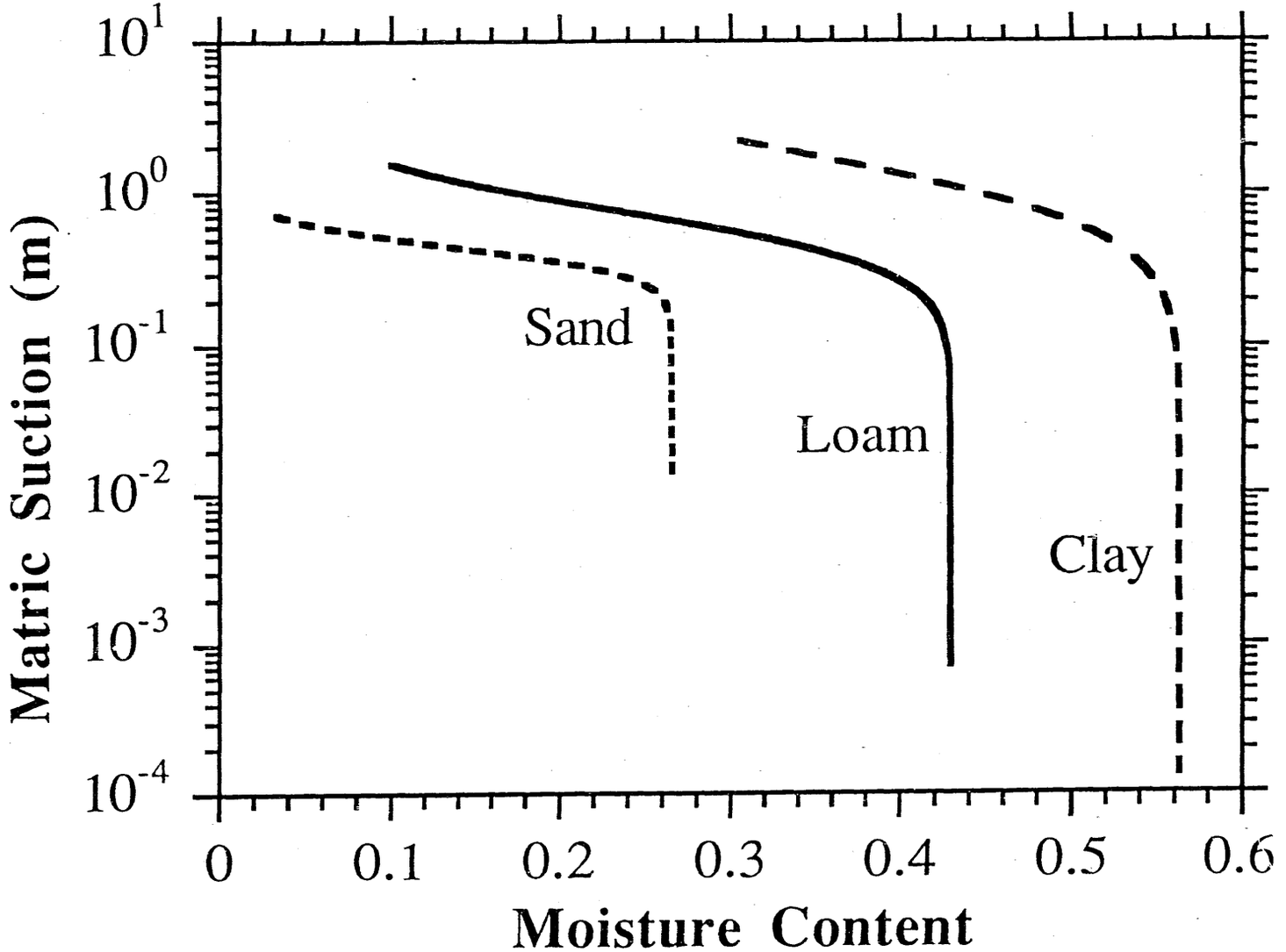
Matric Suction (m)
10^{1}
10^{0}
10^{-1}
10^{-2}
10^{-3}
10^{-4}
Sand
Loam
Clay
0
0.1
0.2
0.3
0.4
0.5
0.6
Moisture Content

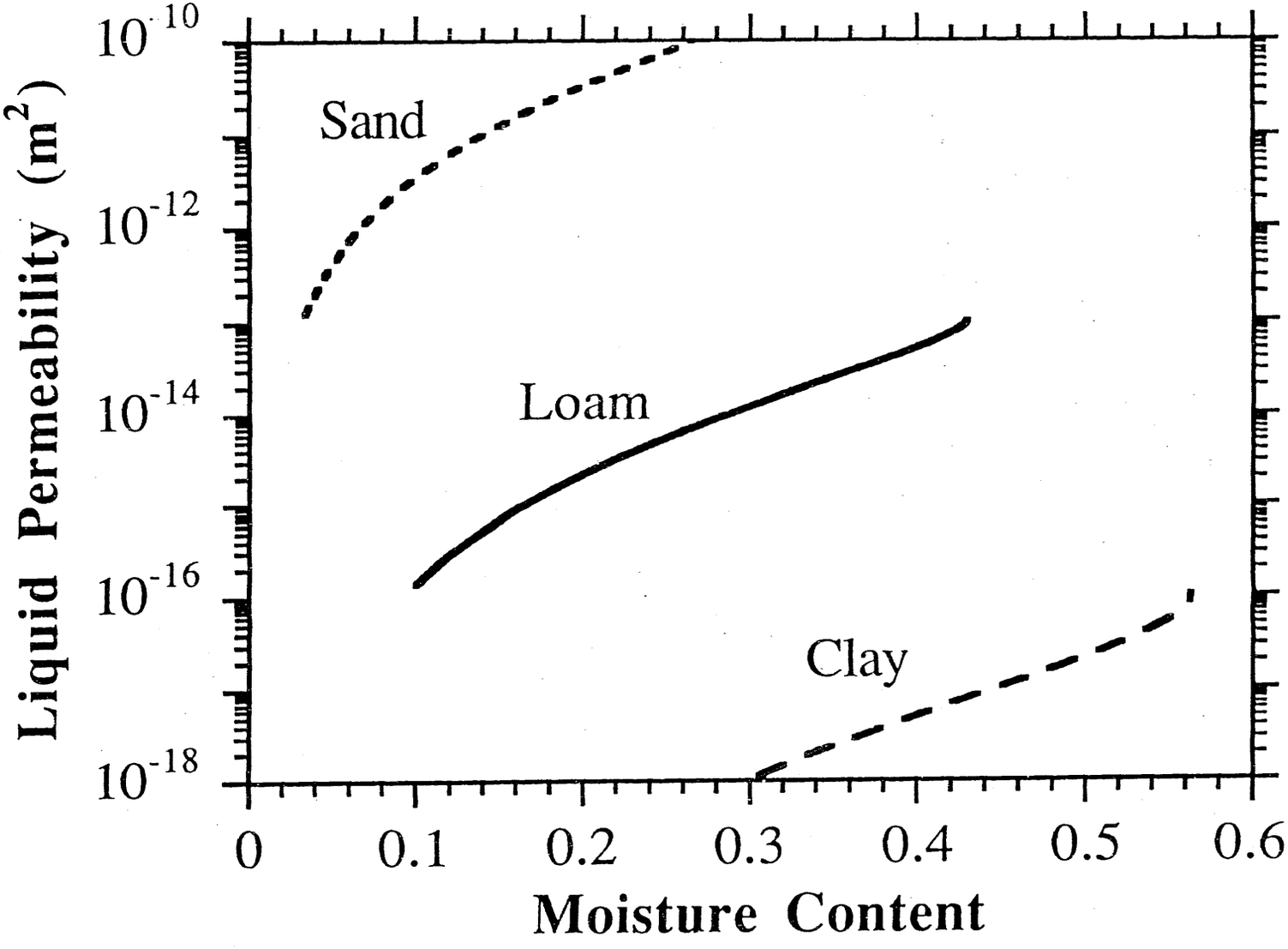
Liquid Permeability (m^2)
10^{-10}
10^{-12}
10^{-14}
10^{-16}
10^{-18}
Sand
Loam
Clay
0
0.1
0.2
0.3
0.4
0.5
0.6
Moisture Content

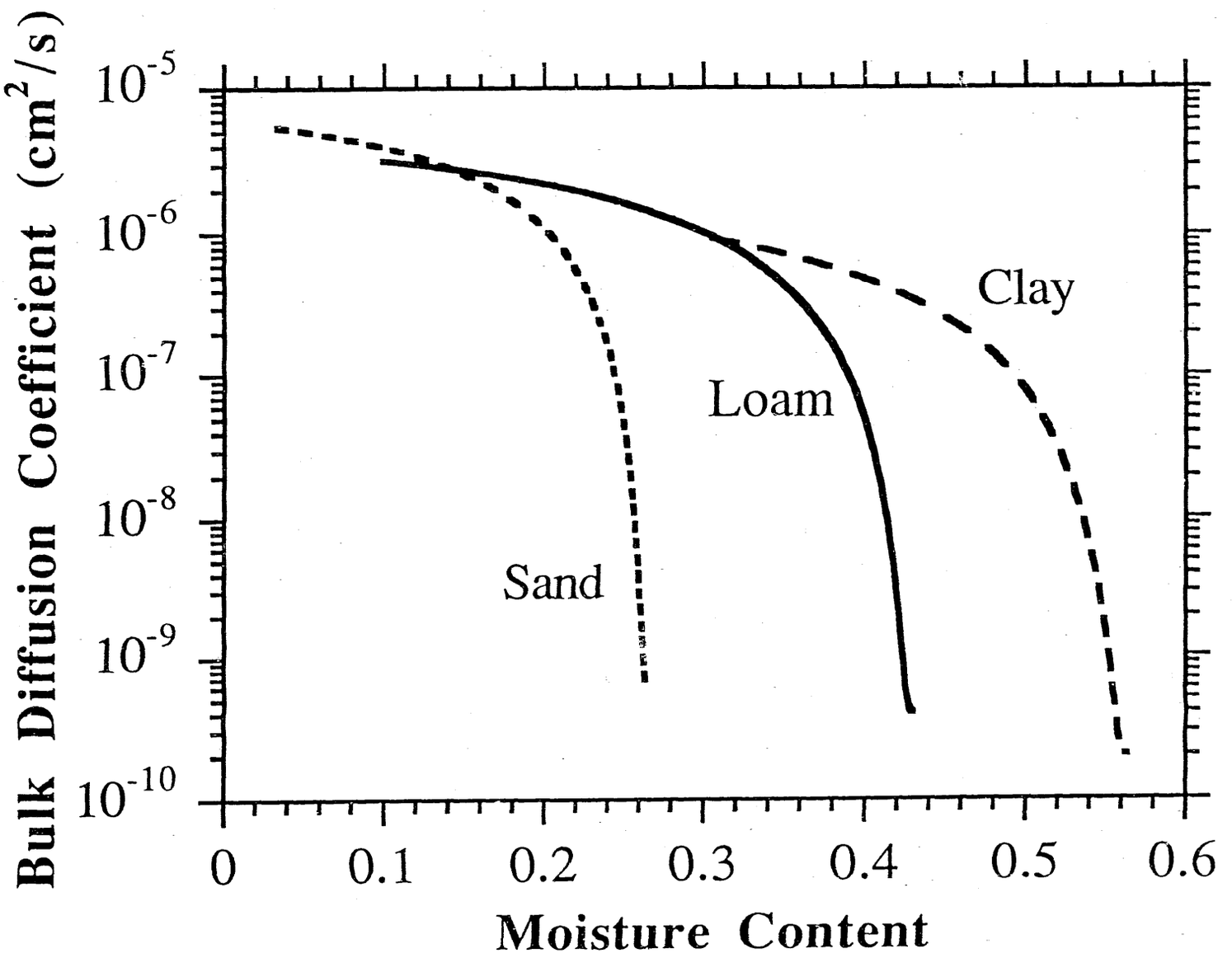
Bulk Diffusion Coefficient (cm²/s)
10⁻⁵
10⁻⁶
10⁻⁷
10⁻⁸
10⁻⁹
10⁻¹⁰
0
0.1
0.2
0.3
0.4
0.5
0.6
Moisture Content
Clay
Loam
Sand

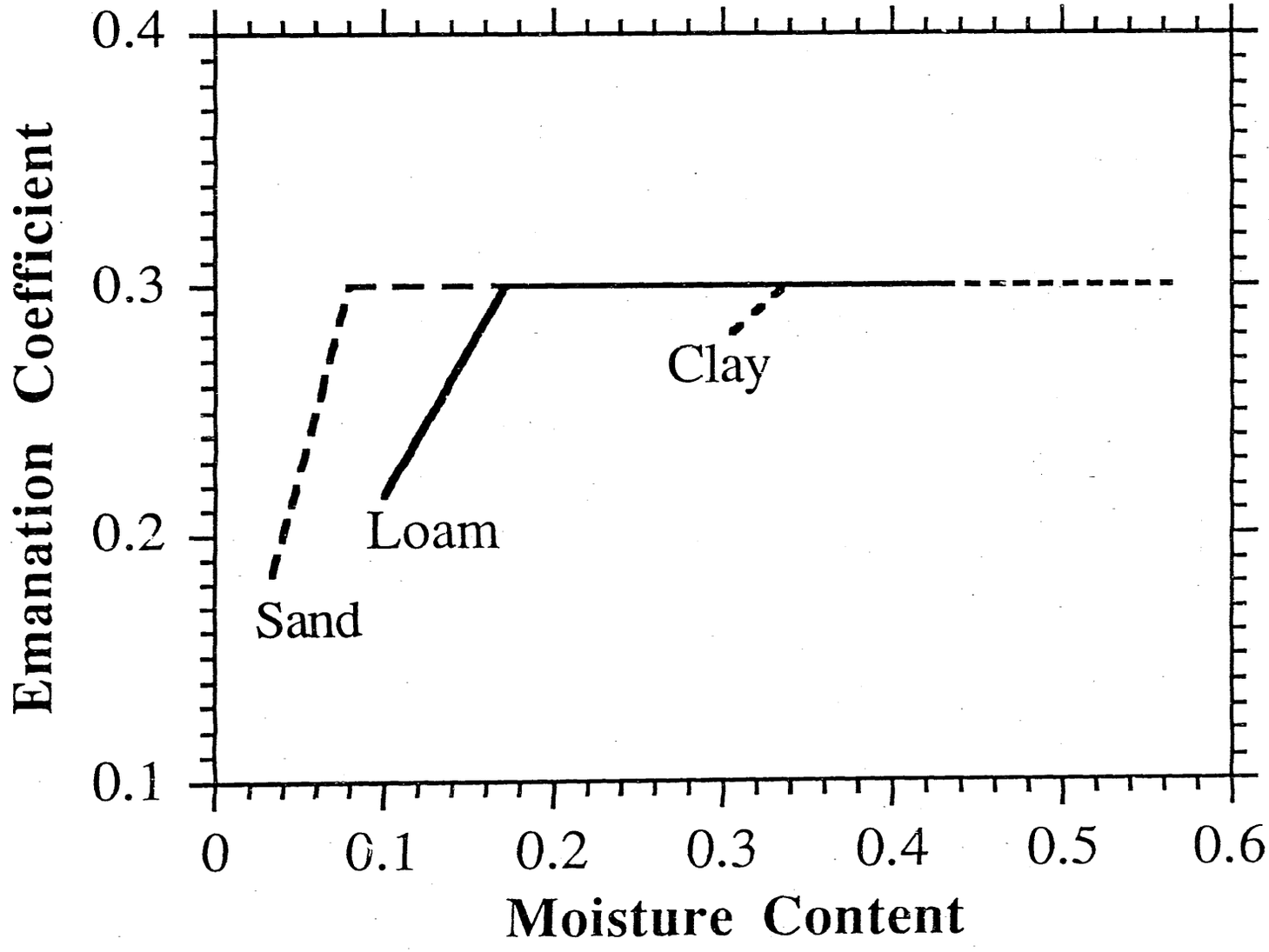
0.4
0.3
0.2
0.1
Emanation Coefficient
Clay
Loam
Sand
0
0.1
0.2
0.3
0.4
0.5
0.6
Moisture Content

Fig

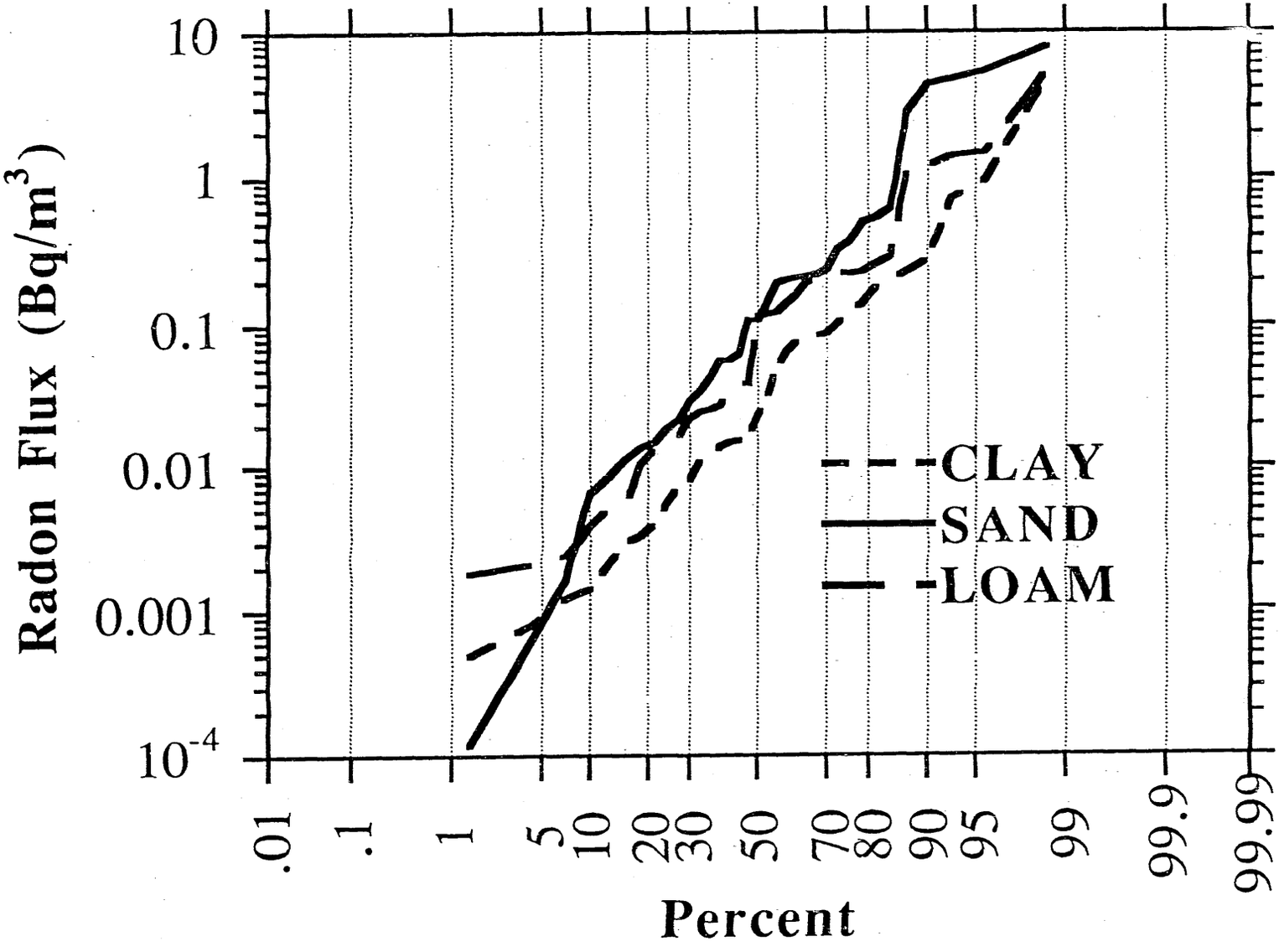
Radon Flux (Bq/m^3)
10
1
0.1
0.01
0.001
10^{-4}
.01
.1
1
5
10
20
30
50
70
80
90
95
99
99.9
99.99
Percent
CLAY
SAND
LOAM

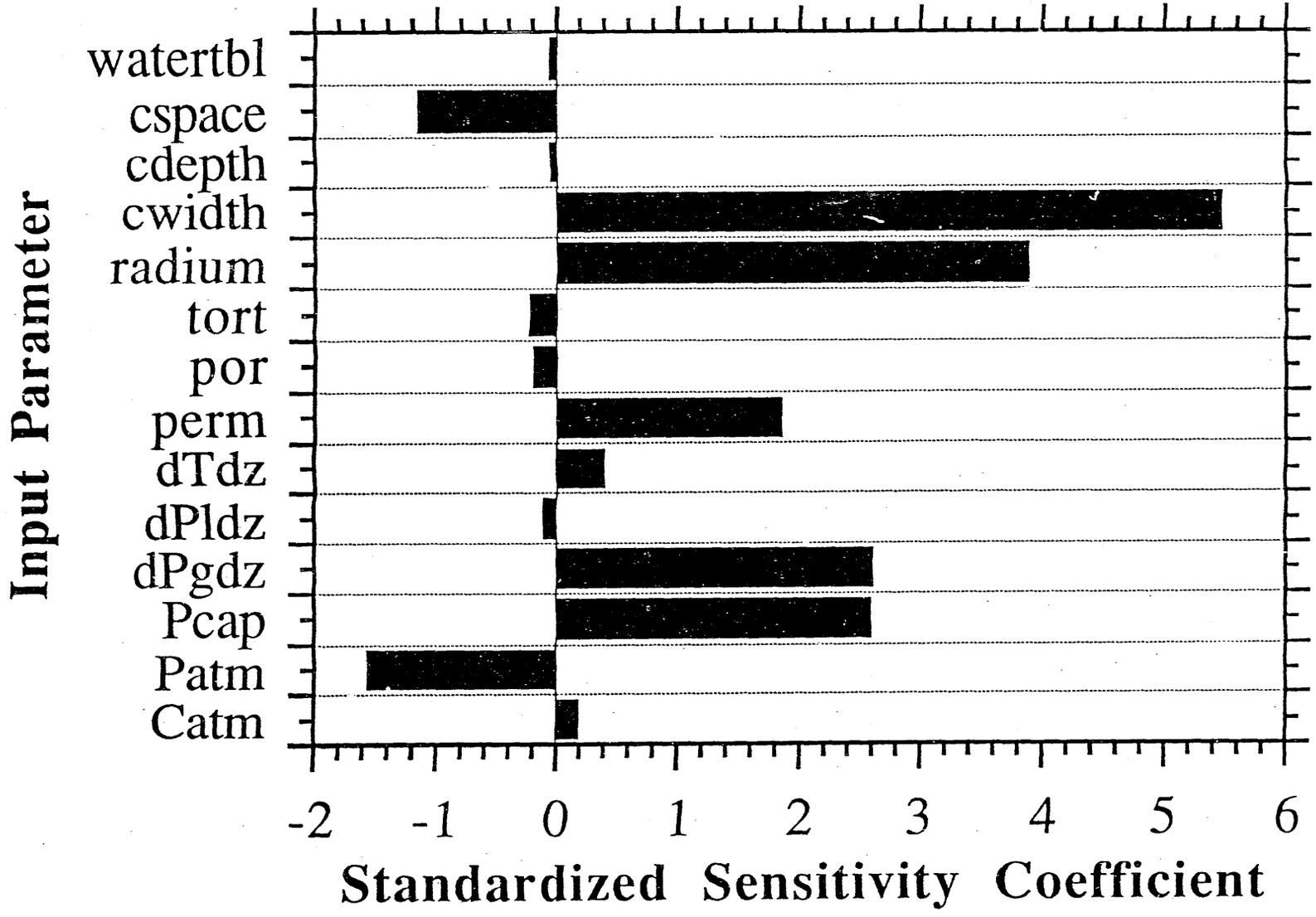
watertbl
cspace
cdepth
cwidth
radium
tort
por
perm
dTdz
dPldz
dPgdz
Pcap
Patm
Catm
Input Parameter
-2
-1
0
1
2
3
4
5
6
Standardized Sensitivity Coefficient

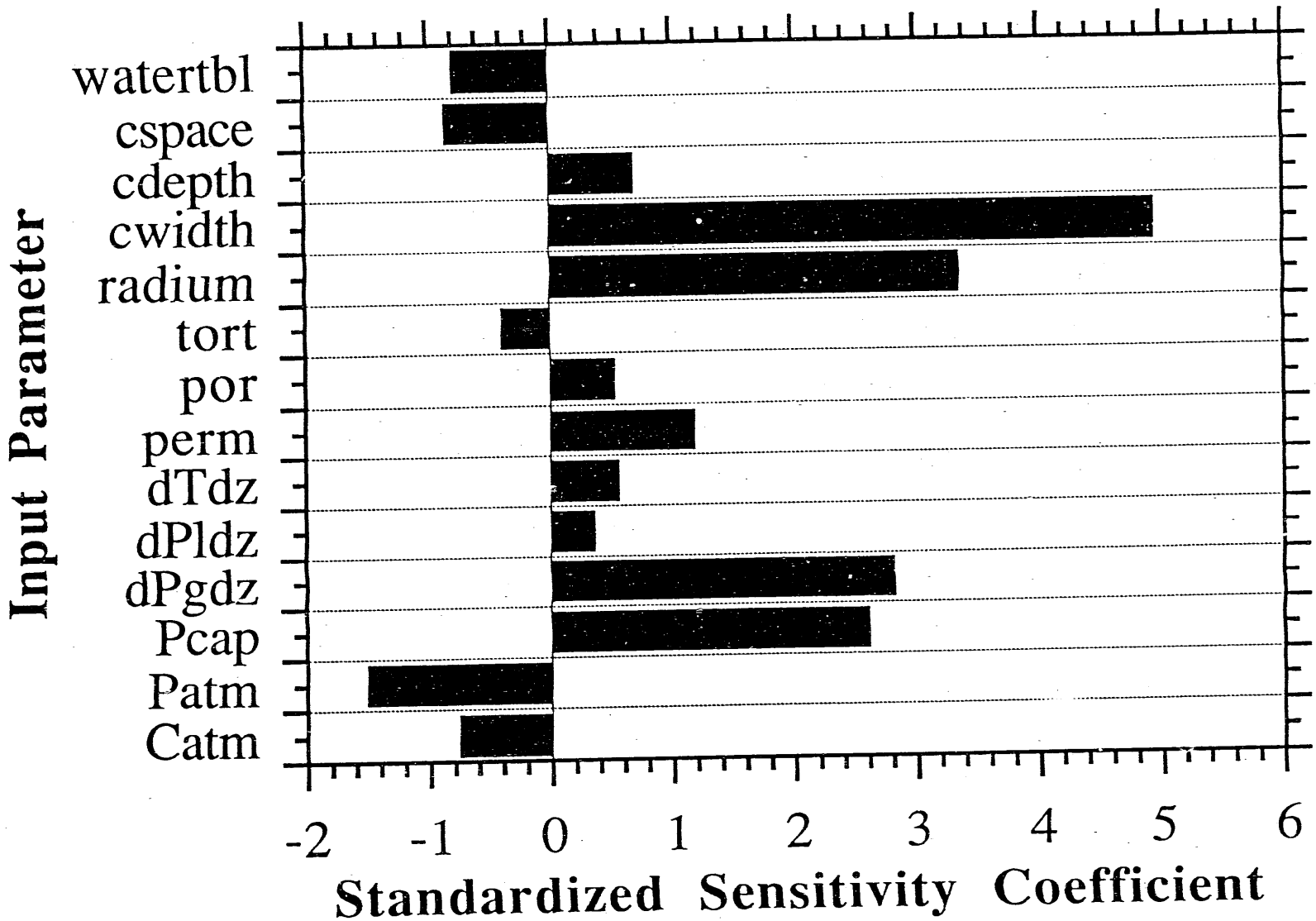
watertbl
cspace
cdepth
cwidth
radium
tort
por
perm
dTdz
dPldz
dPgdz
Pcap
Patm
Catm
Input Parameter
-2
-1
0
1
2
3
4
5
6
Standardized Sensitivity Coefficient

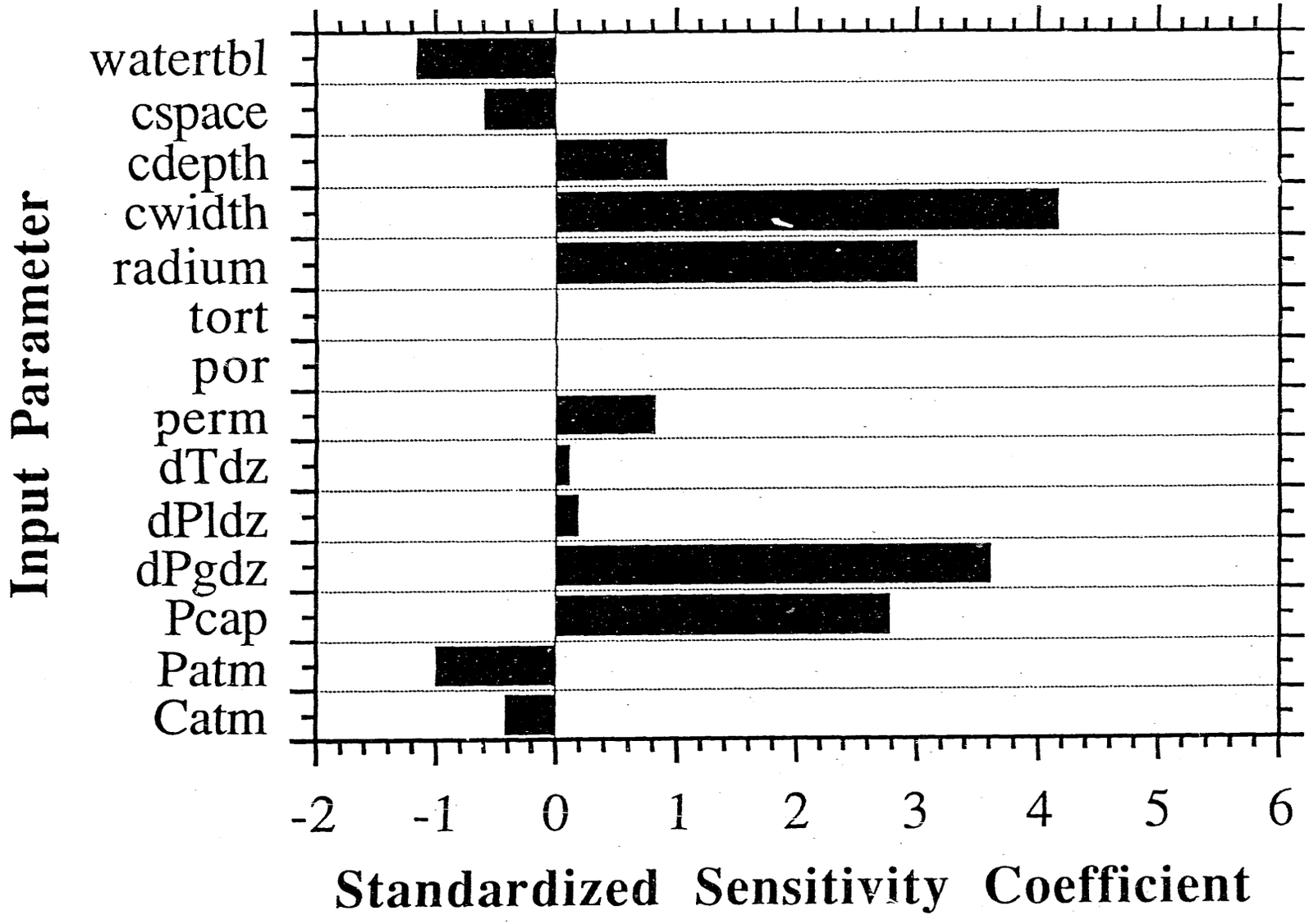
watertbl
cspace
cdepth
cwidth
radium
tort
por
perm
dTdz
dPldz
dPgdz
Pcap
Patm
Catm
Input Parameter
-2
-1
0
1
2
3
4
5
6
Standardized Sensitivity Coefficient

END

DATE FILMED

01 / 23 / 91